

UWB 双方向電波伝搬路モデルを用いた UWB 伝送特性評価の有効性検証

羽田 勝之[†] 高田 潤一^{†,††} 小林 岳彦^{†††}

[†] 東京工業大学大学院理工学研究科 〒152-8550 東京都目黒区大岡山 2-12-1 S6-4

^{††} 独立行政法人情報通信研究機構 医療支援 ICT グループ 〒239-0847 神奈川県横須賀市光の丘 3-4

^{†††} 東京電機大学工学部 〒101-8457 東京都千代田区神田錦町 2-2

E-mail: †{haneda, takada}@ap.ide.titech.ac.jp, ††koba@c.dendai.ac.jp

あらまし 無線通信路においてアンテナと伝搬路を分離してモデル化する方法として、双方向電波伝搬推定法がある。我々は、この方法を超広帯域 (UWB) 無線に応用し、伝搬路の実測およびそれに基づくアンテナに依存しない伝搬モデルの構築を行ってきた。本稿では、双方向電波伝搬路モデルが UWB 伝送特性をどの程度正確に評価可能かについて検討した結果を報告する。伝搬測定より実測した伝達関数および伝搬路モデル化結果より再構成した伝達関数を用いて伝送シミュレーションを行い、両者より得られるビット誤り率特性の差異について考察を行った。伝送方式としては、直接拡散 UWB 方式およびパルス位置変調方式を検討した。この結果、双方向伝搬路モデルは伝送方式によらず実測した伝達関数を用いて得られるビット誤り率特性を正確に再現できることが分かった。ただし、双方向伝搬路推定法の伝搬路モデル化は完全ではなく、フェージングの性質やシンボル間干渉に起因するビット誤り率特性において差異が認められる場合もあった。

キーワード 超広帯域通信, 双方向電波伝搬測定, 双方向電波伝搬路モデル.

Applicability of UWB Double Directional Propagation Modeling for Evaluating UWB Transmission Performance

Katsuyuki HANEDA[†], Jun-ichi TAKADA^{†,††}, and Takehiko KOBAYASHI^{†††}

[†] Graduate School of Science and Engineering, Tokyo Institute of Technology
S6-4, 2-12-1, O-okayama, Meguro-ku, Tokyo 152-8550 Japan

^{††} Medical ICT Group, National Institute of Information and Communications Technology
3-4, Hikarino-oka, Yokosuka-city, Kanagawa 239-0847 Japan

^{†††} Department of Engineering, Tokyo Denki University
2-2, Kanda-nishiki-cho, Chiyoda-ku, Tokyo 101-8457 Japan

E-mail: †{haneda, takada}@ap.ide.titech.ac.jp, ††koba@c.dendai.ac.jp

Abstract This paper investigates the applicability of deterministic ultra wideband (UWB) propagation modeling results for evaluating UWB system performances. The modeling explores the wave propagation characteristics on both transmitting and receiving antenna sides, which is called as the double directional modeling. In evaluating the applicability, bit error probability (BEP) performances were derived by using two kinds of channel impulse responses: 1) raw data which were measured by channel sounding campaign and 2) reconstructed data from the double directional propagation modeling results. In the BEP simulation, direct sequence UWB and pulse position modulation systems were considered. Comparison of the BEP performances from two kinds of channels revealed that the double directional model is capable of evaluating BEP performances accurately. However, it was also found that the limitation of the double directional modeling, such as limited capability of modeling the total received power, affected fading statistics and intersymbol interference properties, and it can lead to different BEP performances in two kinds of simulations.

Key words Ultra wideband, Double directional channel sounding, Double directional propagation modeling.

1. Introduction

Ultra wideband (UWB) technologies have attracted much attention due to its potential to realize high data rate transmission, low-power consumption, and high precision ranging and positioning. In designing and evaluating UWB systems, one must inevitably consider multipath channels. In most UWB transmission simulations, the multipath channels are practically generated by channel models. Here, there are two types of channel models demanded mainly by different purposes: 1) channel models for system design, and 2) channel models for assessing equipment. In the former use, channel models are used to compare the performances of transmission scheme, such as modulation and coding, so that one can state the superiority of the proposed approach. Such models are referred to as standard models, which are represented by IEEE 802.15.3a/4a models [1], [2]. These models are stochastic models which express the channel behaviour based on probability theories. In contrast, testing the performances of equipment under real environments is another demand by product vendors. As that activity requires precise information about channels in which products are installed, channel models should be deterministic models.

We have been conducting UWB deterministic channel sounding and propagation modeling, which analyze propagation behaviours based on physical phenomena. The modeling includes angular characteristics of wave propagation both on the transmitting (Tx) and receiving (Rx) antenna sides. That scheme is called the double directional channel modeling. The analysis is advantageous in two sense: 1) separation of antennas and propagation which leads to the development of antenna-independent channel models is possible [3]. We thus differentiate our modeling results from other channel models by calling it as “propagation models”; and 2) identification of major scattering objects which cause reflection, diffraction, and penetration can be performed (*e.g.*, [4], [5]). However, it is not yet investigated how the double directional propagation models can accurately simulate the performances of UWB systems. This paper presents a comparison of bit error probability (BEP) performances when 1) raw channel transfer function (or equivalently impulse responses), and 2) results of double directional propagation modeling are used. Data transmission simulations using raw channel data is generally called stored channel simulations (*e.g.*, [6], [7]), while the double directional models are derived from the raw channel data.

This paper is organized as follows. Section II will describe the UWB channel sounding campaign where measurement specifications and the double directional propagation modeling is explained. Section III will cover implementation of UWB transmission simulation where we consider direct sequence UWB (DS-UWB) system and pulse position modula-

tion (PPM). Section IV will present results of the simulations and discussions. Finally, Section V will give the conclusion of this paper.

2. UWB Double Directional Channel Sounding Campaign

2.1 Channel Sounding

The double directional UWB channel sounding campaign was conducted in a wooden house. The floor plan of the measurement environment is shown in Fig. 1. The room was almost empty except for desks and displays equipped on the wall. Windows and sliding doors of the room are composed of glass and metal frames. Walls are made up of plaster boards, whereas ceiling and floor consist of wood. In Fig. 1, the position of Tx and Rx antenna are shown. Tx and Rx antennas were mounted 1.30 and 1.00 [m] respectively above the floor. We measured two scenarios with different Tx positions. Scenario I had a line-of-sight to the Rx, while scenario II did not have a line-of-sight component because the door which separates the room and corridor was shut during the experiment. The Tx–Rx distance on the horizontal plane was 5.00 and 5.59 [m] in Scenarios I and II, respectively.

With the use of a vector network analyzer, we measured the channel transfer functions which span from 3.1 to 5.0 [GHz]. Furthermore, by moving antenna position at link ends, we obtained the spatial distribution of channel transfer functions. On the Tx side, 4 antenna positions which realized a synthetic linear array were used, while the Rx side realized a 4×4 rectangular array on the horizontal plane. In total, $4 \times 4 \times 4 = 64$ spatial realizations of channel transfer functions were obtained. Other measurement specifications are summarized in [9].

2.2 Propagation Modeling

The spatial transfer function distribution was then applied to a multi-dimensional channel parameters estimation algorithm, the space alternating generalized expectation and maximization (SAGE) algorithm [8]. The SAGE estimates direction-of-departure (DOD), direction-of-arrival (DOA), propagation time, and complex gain of ray paths. To fully utilize the fine temporal resolution of UWB signals, the path detection was conducted using the power delay profile (PDP). The PDP is defined as the ensemble average of 64 instantaneous channel impulse responses (CIR) in an incoherent manner.

After the propagation parameters were estimated, directivities of the Tx and Rx antennas were compensated from the complex path gain by using the DOD and DOA information. Tx and Rx antenna directivities were measured prior to the channel sounding in an anechoic chamber. The resultant complex path gain ideally expresses only propagation characteristics.

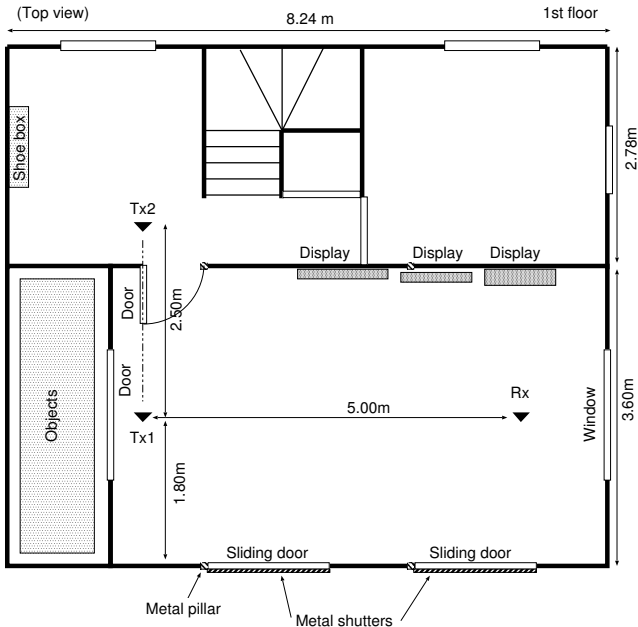
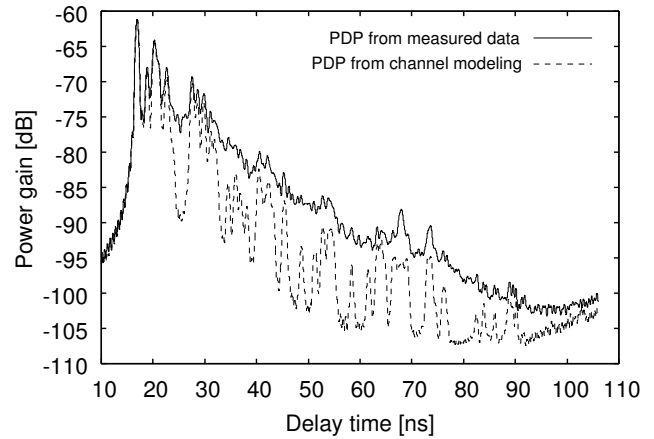


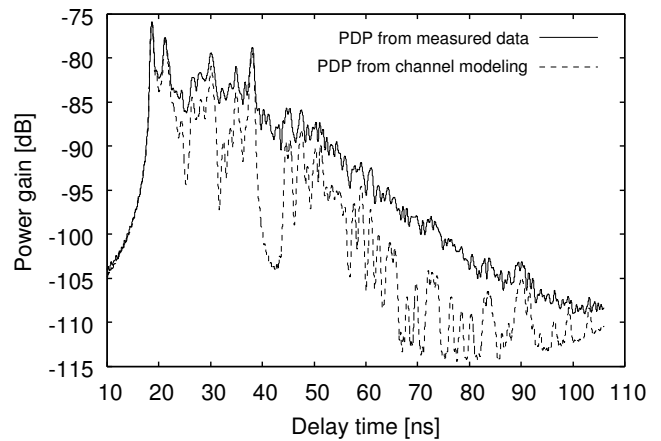
Figure 1 Floor plan of the UWB channel sounding campaign in a home environment.

2.3 Modeling Results

In Fig. 2, we show the PDP derived from the raw channel data and reconstructed from the double directional models. In reconstructing the CIR from the double directional propagation models, we assumed the same antennas as we used in the measurement at both sides of the link. According to Fig. 2, the double directional models does not reconstruct the original PDP properly. The strong multipath components which appears in the short delayed areas were modeled well, while modeling weaker paths in the long delayed areas was more difficult. This is simply due to the dynamic range of the paths over noise level. However, it was also found that paths with high signal-to-noise ratio were not always able to be detected. For example, looking at the PDP of Scenario I, PDP from the double directional models failed to reconstruct the responses with delay time around 26 ns. Paths in the area never appear as a peak in the PDP probably because they are hidden by sidelobes of the adjacent peaks with higher power appearing around 23 and 28 [ns]. The same holds for the PDP obtained from Scenario II with delay time around 40 ns. The limited extraction of power is essentially due to the double directional modeling which is particularly accomplished by the SAGE. As the SAGE requires an underlying model in estimating propagation parameters, such as the wavefront model of impinging waves, the accuracy of the model largely affects the amount of extracted power [8]. In Scenario I, the double directional modeling could extract 75 % of the total received power, while it revealed even a lower value in Scenario II, 55 %. In fact, the more complicated the environment is, the smaller the percentage of modeled power is expected [9]. Similar observations from channel sounding cam-



(a) Scenario I.



(b) Scenario II.

Figure 2 PDP derived from raw channel data (solid line). PDP reconstructed from the double directional propagation models is overlaid (dashed line).

paigns are reported by several researchers, such as Molisch et al. [10], Thomä et al. [11], and Win and Scholtz [12], all of which utilized a model-based propagation parameter estimation scheme like SAGE. Modeling of the residual component has been done using the exponential decay of the power delay profile [11], but we exclude this components in later analyses to simplify discussions.

The transmission simulation which shall be described in the next Section will use 64 instantaneous CIR from the measurement, and that from the double directional modeling results. In deriving CIR, we applied a -105 dB threshold level to eliminate noise. If amplitude of the CIR was below the threshold, the value was padded with zeroes.

3. UWB Transmission Simulation

We conducted UWB transmission simulations using stored channels and double directional propagation models. In this

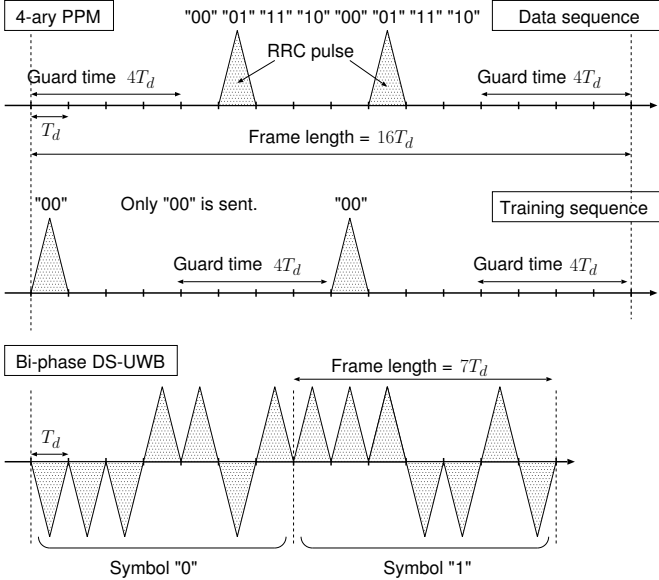


Figure 3 Frame format of the UWB transmission simulations for 4-ary PPM and bi-phase DS-UWB systems.

simulation, we considered 4-ary PPM and bi-phase DS-UWB systems which are actually implemented in [13]. Both modulations use a root-raised cosine (RRC) pulse as a unit pulse which spans from 3.1 to 5.0 [GHz]. Duration of the RRC pulse, T_d , was set either to 2.4 or 4.8 [ns]. The PPM conveys information by the position of RRC pulse. In DS-UWB, a spread sequence of $[+1 +1 +1 -1 -1 +1 -1]$ was used where each chip was represented by the RRC pulse, leading to the frame length of $7T_d$. Information is mapped on the polarity of the spread sequences. Frame format of data sequence is depicted in Fig. 3. The data frame of PPM contains guard time, and each symbol is sent twice. Thus the frame length of the PPM simulation results in $16T_d$. Differential encoding was used to map information bits to waveforms in DS-UWB systems. It enables us to combat the inversion of waveform polarity due to propagation channels, which degrades the BEP performance. In Fig. 3, the frame format of training signals are also shown. It consists of 1334 frames, and is sent before sending the data stream so that the receiver is synchronized with the transmitter. In PPM implementation, the position of the guard time for the training sequence is different from that of the data sequence, and only “00” is transmitted. In the DS-UWB system, the training sequence consists only of the symbol “0”. To simplify the simulation conditions, perfect synchronization was assumed, and channel coding was not taken into account.

On the Rx side, a correlation receiver is implemented. It finds a symbol that maximizes the correlator output between the receiving waveform and the reference waveform which corresponds to each symbol.

The simulation flow is depicted in Fig. 4. The flow emulates the structure of an actual testbed [13]. We defined that

an RRC pulse is transmitted from the RF frontend defined at point “A” of Fig. 4 which equivalently means that characteristics of power amplifier and RF filter is compensated. On the receiving side, we multiplied the receiving waveform from the Rx antennas by the transfer function of an RF filter and a low-noise amplifier (part “B” in Fig. 4) which is actually measured from the equipment [13]. Noise level inside the receiver was also determined by that of a Digital Sampling Oscilloscope equipped on the Rx side.

4. Simulation Results

In this section, results of BEP simulations are described. Here we define two BEPs for the evaluation: 1) BEP obtained from 64 spatial realizations in one scenario which we will call “local BEP”, and 2) averaged BEP over the 64 realizations which will be referred to as “average BEP”.

Figures 5 and 6 show the average BEP characteristics dependent on energy per bit, E_b/N_0 , for Scenarios I and II, respectively. In each figure, two sets of curves corresponding to $T_d = 2.4$ and 4.8 ns are shown. Furthermore, BEP curve from stored channel simulations and double directional models are shown in the same chart for comparison. As a baseline, the BEP curve assuming additive white gaussian noise (AWGN) channel is overlaid. It must be noted that the E_b/N_0 in these figures is defined as the E_b/N_0 of the stored channel simulations. E_b/N_0 of the double directional models are treated as the same E_b/N_0 of the corresponding stored channel simulations from which the double directional models are derived. The purpose for this definition is to analyze the impact of the multipath components extracted by the double directional modeling to the BEP performance.

Every figure shows that the BEP is decreasing with the increase of E_b/N_0 when $T_d = 4.8$ ns. In contrast, when $T_d = 2.4$ ns, the BEP curve reveals a floor effect in the higher E_b/N_0 areas. This is due to intersymbol interference (ISI) which tends to be more severe when the symbol length is shorter. As an exception, the PPM modulation from the stored channel simulation in Scenario II reveals floor effect even when $T_d = 4.8$ ns.

When comparing the BEP characteristics from the stored channel simulations and those from the double directional models, the following observations were obtained:

(1) In Scenario I, the BEP from the double directional modeling is always less than the BEP from the stored channel simulations. The difference in the slope of the two curves is attributed to the limited capability to extract the total received power by the double directional models. As we discussed in Section II using the PDP, the double directional models successfully characterized the LOS components, while other multipath components were not properly modeled. This results in different power ratio between the LOS and other multipath components. Here it is convenient

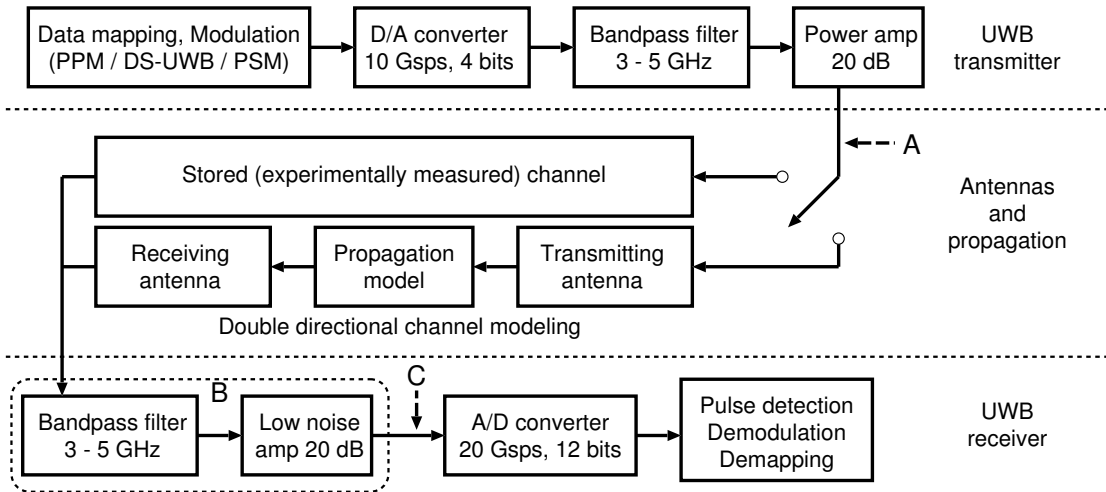
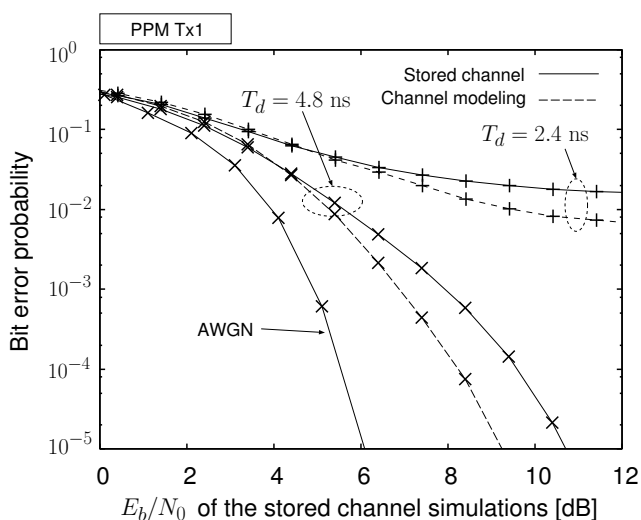
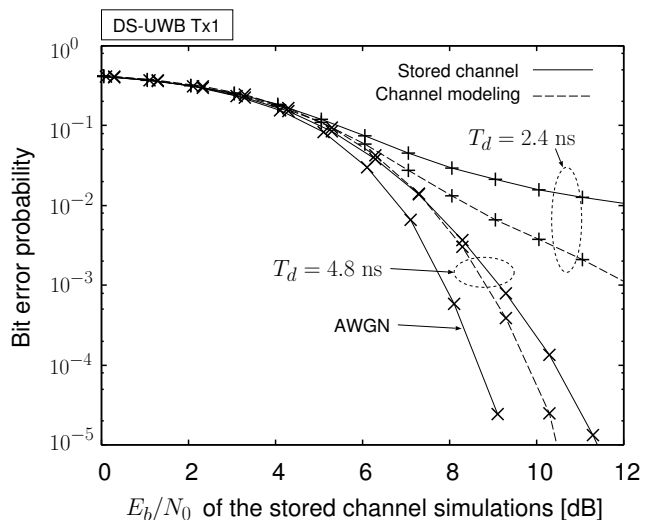


Figure 4 Block diagram of the UWB transmission simulation using stored channels and double directional propagation models.



(a) 4-ary PPM.



(b) Bi-phase DS-UWB.

Figure 5 E_b/N_0 versus average BEP for Scenario I.

to introduce the Rician K -factor [14] to discuss it. The double directional modeling derived a higher K than the stored channels. Thus the BEP curve from the double directional models approaches the BEP characteristics of AWGN channels where K is infinity.

(2) In the PPM results in Scenario II with $T_d = 4.8$ ns, the BEP curve from the stored channel simulation shows the floor effect in high E_b/N_0 due to ISI, while the effect is not found in the double directional modeling. The difference can be interpreted again as the limited performances of the double directional modeling in detecting multipath components. It was found that only 3 out of 64 local BEP revealed the floor effects in the stored channel simulations, while all the local BEP in the double directional modeling decreased to 0. As a result, the three “nonzero” local BEP caused the difference. The same observation holds for the DS-UWB in

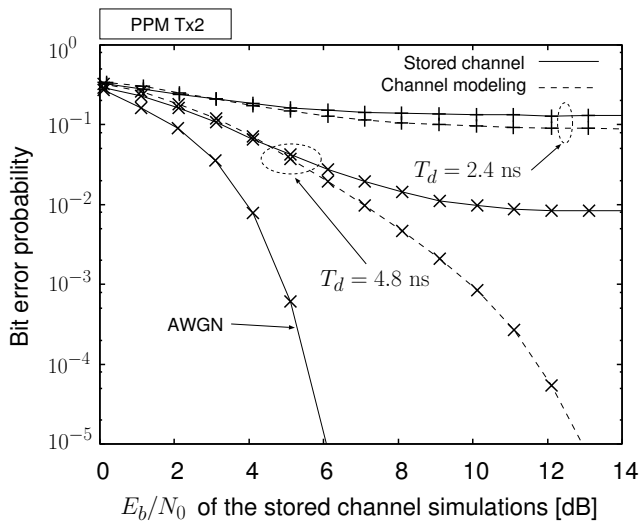
Scenario I, $T_d = 2.4$ ns.

(3) Other than the differences mentioned in 1) and 2), the BEP curve from the double directional modeling is close to that from stored channel simulations. Particularly, the saturated BEP in the high E_b/N_0 areas is accurately determined regardless of modulation schemes in most cases.

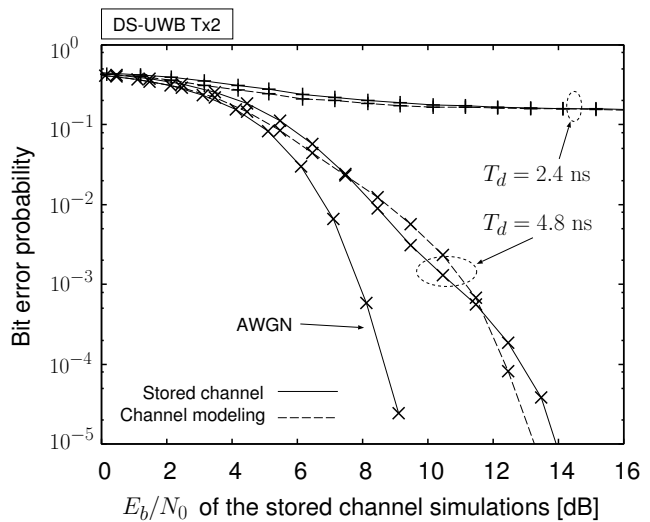
It is concluded from the above observations that predicting the BEP performances can be accurately performed when ISI oriented errors are dominant, or when the transmission data rate is sufficiently low such that the system does not suffer from ISI. In contrast, differences can result in two curves when part of the local BEP is subjected to ISI, while the other is ISI free.

5. Conclusion

This paper investigated the applicability of the double di-



(a) 4-ary PPM.



(b) Bi-phase DS-UWB.

Figure 6 E_b/N_0 versus average BEP for Scenario II.

rectional propagation modeling for evaluating BEP performances. Comparison of the BEP from the double directional models with that from stored channel simulations demonstrated that even if the double directional models characterize limited portion of the total received power, the model is still capable of predicting the average BEP performances as accurately as stored channel simulations. The limited power of the double directional models appears in the slope of BEP curves if the system does not suffer from ISI. In addition, if some of the local BEP suffers from ISI while the rest is free from ISI, the difference between two curves can be more significant.

For further agreement of average BEP performance with stored channel simulations, improvement of the double directional modeling to extract more received power is planned.

Acknowledgment

The authors would like to thank members of the NICT UWB Consortium for valuable helps in the experiment and discussions. This research is also partly supported by the Japan Society for the Promotion of Science Research Fellowships for Young Scientists.

References

- [1] J. Foerster et al. "Channel modeling sub-committee report (final)," IEEE P802.15-02/490r1-SG3a, Feb. 2003.
- [2] A. F. Molisch et al. "IEEE 802.15.4a channel model – final report," IEEE P802.15-04/662r0-SG4a, Nov. 2004.
- [3] M. Steinbauer, A. F. Molisch, and E. Bonek, "The double directional radio channel," *IEEE Antennas and Propagat. Mag.*, vol. 43, no. 4, pp. 51–63, Aug. 2001.
- [4] K. Haneda, J. Takada, and T. Kobayashi, "Double directional ultra wideband channel characterization in a line-of-sight home environment," *IEICE Trans. Fundamentals*, E88–A, no. 9, pp. 2264–2271, Sep. 2005.
- [5] K. Kalliola, H. Laitinen, P. Vainikainen, M. Toeltsch, J. Laurila, and E. Bonek, "3-D double-directional radio channel characterization for urban macrocellular applications,"

- IEEE Trans. Antennas Propagat.*, vol. 51, no. 11, pp. 3122–3133, Nov. 2003.
- [6] K. Takizawa, S. Fujita, Y. Rikuta, K. Hamaguchi, and R. Kohno, "Measurement based performane evaluation of a 26 GHz band UWB communication system," to appear in *Proc. 64th IEEE Veh. Tech. Conf.*, Montreal, Canada, Sep. 2006.
- [7] J. Keignart, C. Abou-Rjeily, C. Delaveaud, and N. Daniele, "UWB SIMO channel measurements and simulations," *IEEE Trans. Microwave Theory Tech.*, vol. 54, no. 4, pp. 1812–1819, Apr. 2006.
- [8] K. Haneda, J. Takada, and T. Kobayashi, "A parametric UWB propagation channel estimation and its performance validation in an anechoic chamber," *IEEE Trans. Microwave Theory Tech.*, vol. 54, no. 4, pp. 1802–1811, Apr. 2006.
- [9] K. Haneda, J. Takada, and T. Kobayashi, "Cluster properties investigated from a series of ultra wideband double directional propagation measurements in home environments," *IEEE Trans. Antennas Propagat.*, to be published in Dec. 2006.
- [10] A. F. Molisch, M. Steinbauer, M. Toeltsch, E. Bonek, and R. S. Thomä, "Capacity of MIMO systems based on measured wireless channels," *IEEE J. Select. Areas Commun.*, vol. 20, no. 3, pp. 561–569, Apr. 2002.
- [11] R. S. Thomä, M. Landmann, A. Richter, and U. Trautwein, *Multidimensional High-Resolution Channel Sounding*. in *Smart Antennas in Europe – State-of-the-Art*, EURASIP Book Series, Hindawi Publishing Corporation, New York, USA, 2005.
- [12] M. Z. Win and R. A. Scholtz, "Characterization of ultra-wide bandwidth wireless indoor channels: a communication-theoretic view," *IEEE J. Select. Areas Commun.*, vol. 20, no. 9, pp. 1613–1627, Dec. 2002.
- [13] K. Takizawa, I. Nishiyama, and Y. Rikuta, "UWB testbed for evaluating various UWB systems and waveforms", IEICE Tech. Rep., WBS2004–08, SAT2004–32, Apr. 2004 (In Japanese).
- [14] R. Vaughan, and J. B. Andersen, *Channels, Propagation and Antennas for Mobile Communications*. The IEE Press, London, UK, 2003, pp. 706–707.